DOI: 10.1002/ejoc.201201631

Synthesis, Electrochemistry, and Hierarchical Self-Organization of Fulleropyrrolidine–Phthalimide Dyads

Aleksandra Mitrović,[a] Nina Todorović,[b] Andrijana Žekić,[c] Dalibor Stanković,[d] Dragana Milić,[a] and Veselin Maslak*[a]

Keywords: Electrochemistry / Cyclic voltammetry / Fullerenes / Microwave chemistry / Dyads / Polymorphism

A series of novel fulleropyrrolidine–phthalimide dyads was synthesized and their electrochemical and self-assembly properties were investigated. Efficient synthesis of acceptor–acceptor dyads was performed under microwave irradiation. Fine-tuning of the second redox potentials in the dyads was achieved by varying the length of the aliphatic spacer (C_2 to C_{12}) between the fulleropyrrolidine and phthalimide moieties. Shape-shifting and supramolecular polymorphism were observed for these compounds during self-assembly.

Introduction

Since its discovery[1] and the development of a large-scale preparative method,[2] C_{60} fullerene has proven to be an indispensable building block for the synthesis of tailor-made materials with unique and tunable electronic, magnetic, and optical properties. As it is very amenable to an extensive range of covalent modifications, much research effort has been devoted to this field. One of the most explored methods for the functionalization of fullerene is its 1,3-dipolar cycloaddition to azomethine ylides (Prato reaction) to yield fulleropyrrolidines with different structures and solubilities.[3–7]

Fullerene-based dyads provide a means of fine-tuning the electrochemical properties of fullerene-based materials. Dyads are composed of electron-donor or electron-acceptor units covalently attached to the core of C_{60}. In the dyad, fullerene displays unique electronic properties as a strong electron acceptor. Most of the C_{60} derivatives, including fulleropyrrolidine, present electron-acceptor properties that are poorer than those of parent C_{60} as a consequence of the saturation of a double bond of the C_{60} framework, which raises the energy of the LUMO.[8] Different strategies have been explored to increase the electron-accepting character of fullerene derivatives within C_{60}-based dyads: 1) electron-acceptor moieties covalently attached to C_{60}, 2) electronegative atoms directly linked to C_{60}, 3) periconjugative effects, 4) pyrrolidinium salts, 5) heterofullerenes, 6) fluorofullerenes, and 7) endohedral fullerenes.[9–11] Introducing quinoidal subunits as an electron-accepting group[12,13] usually results in decreased electronegativity of the fullerene part in comparison to parent C_{60}. However, the introduction of much stronger electron-withdrawing groups such as in the case of cyano- and carbethoxymethanofullerenes resulted in enhanced electron-accepting properties.[14] Thus, the overall electrochemical properties of the dyad depend on the electroactivity of each one of its constituents. In addition, the distance between the two parts of the dyad can also have an influence.[13]

Fullerene-based dyads have the ability to undergo hierarchical self-assembly, which makes them attractive for the preparation of materials with a variety of supramolecular architectures showing numerous functions and applications.[15–18] The process of self-organization in nano- and microarchitectures is governed by a fine balance between different intermolecular forces such as π–π stacking interactions of the curved C_{60} surface and van der Waals interactions.[19–21] Self-assembly of functionalized fullerene dyads has been studied in solution, on surfaces, and by the drop-drying process.[22,23] The molecular design of dyads has been recognized as crucial for the creation of functional assemblies and soft materials with excellent optoelectronic properties.[16]

Wit the aim to obtain novel fullerene-based materials with controllable electric and self-assembly properties, we synthesized a series of fulleropyrrolidine dyads containing covalently linked phthalimide as an electron-acceptor group with aliphatic spacer units ranging from C_2 to C_{12} in length (Figure 1).

[a] Faculty of Chemistry, University of Belgrade, Studentski trg 16, P. O. B. 51, 11158 Belgrade, Serbia
Fax: +381-11-2184330
E-mail: vmaslak@chem.bg.ac.rs
Homepage: http://www.chem.bg.ac.rs/osoblje/43-en.html
[b] ICTM, Center for Chemistry, University of Belgrade Njegoševa 12, 11000 Belgrade, Serbia
[c] Faculty of Physics, University of Belgrade, Studentski trg 12, 11000 Belgrade, Serbia
[d] Innovation Center of the Faculty of Chemistry, Studentski trg 12, 11000 Belgrade, Serbia
Supporting information for this article is available on the WWW under http://dx.doi.org/10.1002/ejoc.201201631.

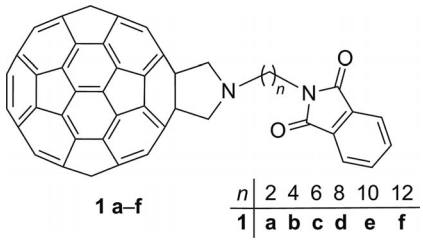

Figure 1. Structures of the synthesized fulleropyrrolidine–phthalimide dyads.

The electrochemical properties and the self-assemblies of fulleropyrrolidine–phthalimide dyads **1a**–**f** were investigated. Furthermore, during the course of this study, a microwave-assisted synthesis was employed to significantly improve the overall synthetic process.

Results and Discussion

Synthesis

Compounds **1a**–**f** (Figure 1) were prepared by the general synthetic strategy summarized in Scheme 1. The preparation of key intermediates **6a**–**f** was based on Prato's reaction.[3–5] Appropriate amino acids **4a**–**f** were prepared starting from Boc-protected diamines **2a**–**f**. These amines were alkylated with benzyl bromoacetate (BBA) to obtain corresponding glycine benzyl esters **3a**–**f**. Selective deprotection of **3a**–**f** at the carboxylic function afforded amino acids **4a**–**f**. These α-amino acids were allowed to react with formaldehyde and C_{60} in refluxing toluene to form *N*-Boc-protected amino fulleropyrrolidines **5a**–**f** in 21–36% yield. Finally, key intermediates **6a**–**f** were obtained in nearly quantitative yields after deprotection of **5a**–**f** by using 2,2,2-trifluoroacetic acid (TFA) in CH_2Cl_2.

Fulleropyrrolidine–phthalimide dyads **1a**–**f** were obtained by reaction of corresponding amino fulleropyrrolidine **6a**–**f** and phthalic anhydride. Firstly, the reaction was performed by conventionally heating a mixture of **6f** and phthalic anhydride in AcOH/pyridine (3:2). The desired product was obtained in 16% yield after heating at 120 °C for 4 h (result not shown). To decrease the reaction time and to increase the yield of the target compounds, we investigated the applicability of microwave irradiation for the fulleroamine/phthalic anhydride coupling (Scheme 1). It is well known that microwave-assisted organic synthesis has some advantages over conventional methods: remarkable decrease in the reaction times and improved isolated yields of the products. Previously, microwave irradiation was successfully applied in cycloaddition reactions to C_{60};[24,25] however, a retro-Prato reaction of the fulleropyrrolidines was also achieved.[26,27] When mixtures of fulleroamines **6a**–**f** and phthalic anhydride dissolved in AcOH/pyridine (3:2) were irradiated in a Mycrosynth reactor (E = 300 W) for 30 min, appropriate fulleropyrrolidine–phthalimide dyads **1a**–**f** were obtained in good yields (40–59%). Relative to values obtained by conventional heating, a reaction time that was sixfold shorter and a yield that was threefold greater were achieved for **1f**.

Electrochemical Study

All novel compounds reported in this work are composed of two differently spaced electroactive moieties, namely, a fulleropyrrolidine and a phthalimide (Figure 2). Their electrochemical properties were studied by cyclic voltammetry (CV) in dimethylformamide (DMF) at room temperature by using nBu$_4$NPF$_6$ as a supporting electrolyte, a glassy carbon electrode as the working electrode, and the Fc/Fc$^+$ couple as an internal standard (see the Experimental Section). All compounds gave CV curves that were similar in shape with notable differences in the positions of the second reduction wave. For reasons of clarity, only one CV curve is presented in Figure 2, whereas the half-wave redox potentials of all tested compounds are given in Table 1. In all cases, including the *N*-methylfulleropyrrolidine (NMF)

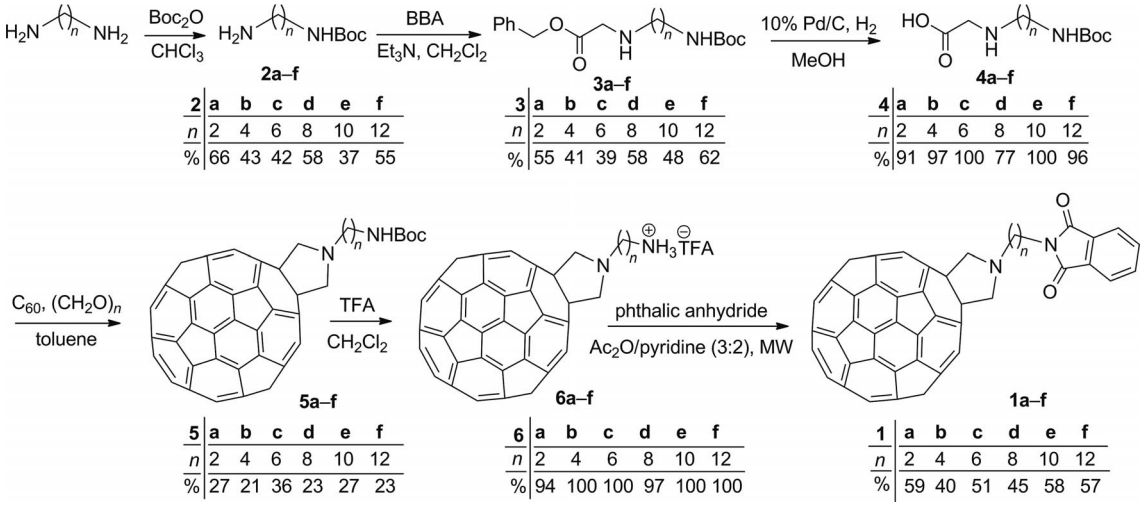

Scheme 1. Synthetic route to fulleropyrrolidine–phthalimide dyads **1a**–**f**.

and *N*-benzylphthalimide (NBP) model compounds, the sample concentration was 1 mM. Six reduction peaks were observed in the CV curve of **1a**, which are labeled by increasing Roman numerals (Figure 2). The reduction potentials for the model compounds were used to assign the redox peaks ($E_{1/2}$ values) in the cyclic voltammograms of **1a**–**f** (Table 1). Fulleropyrrolidine–phthalimide dyads **1a**–**f** all showed four reversible one-electron reduction waves attributable to the fullerene moiety and located at ca. –1, –1.5, –2, and –2.6 V (I, II, IV, and V, respectively; Figure 2). In addition, another two reversible one-electron reduction peaks were observed at ca. –2 and –2.9 V, which correspond to the reduction of the phthalimide addend (III and VI, respectively; Figure 2).

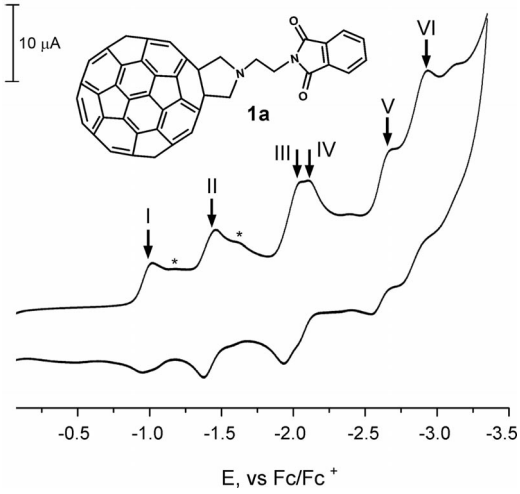

Figure 2. CV curve of **1a** at 100 mV s^{-1} in DMF containing 0.1 M nBu$_4$NPF$_6$.

Table 1. Electrochemical reduction data (in V vs. Fc/Fc$^+$) for fulleropyrrolidine–phthalimide dyads.

Compd.	$E_{1/2}$(I)	$E_{1/2}$(II)	$E_{1/2}$(III)	$E_{1/2}$(IV)	$E_{1/2}$(V)	$E_{1/2}$(VI)
1a	–1.02	–1.50	–2.02	–2.12	–2.66	–2.91
1b	–1.02	–1.53	–2.02	–2.10	–2.61	–2.92
1c	–1.01	–1.56	–1.99	–2.11	–2.62	–2.91
1d	–1.02	–1.58	–1.99	–2.07	–2.62	–2.87
1e	–1.00	–1.59	–1.99	–2.11	–2.61	–2.89
1f	–1.01	–1.62	–2.02	–2.10	–2.62	–2.92
NMF	–0.91	–1.41		–2.05	–2.76	
NBP			–2.02			–2.93

The first one-electron reductions for **1a**–**f** correspond to the first reduction of the fulleropyrrolidine. For all derivatives, the $E_{1/2}$(I) values are shifted by 90–110 mV to more negative potentials relative to that of parent NMF (Table 1). The next reduction peak was also a one-electron process located on C_{60}, and the $E_{1/2}$(II) values were gradually shifted to more negative potentials (–1.50 to –1.62 V); the largest shift was exhibited by **1f** (Table 1). A gradual decrease in the second reduction potential with a decrease in the length of the alkyl spacer indicates the importance of the proximity of the fullerene and phthalimide moieties and could be a consequence of noncovalent interactions between the fulleride anion and the electron-accepting phthalimide moiety. Under the applied CV conditions, shoulders close to waves $E_{1/2}$(I) and $E_{1/2}$(II) appeared, probably as a result of the slight decomposition of the investigated compounds (labeled by asterisks, Figure 2). The third and fourth reduction peaks are overlapping and belong to the reductions of NBP and NMF (–2.02 and –2.05 V, respectively). The fifth and the sixth reduction potentials, which are similar between derivatives and to the parent compounds, correspond to the forth reduction of fullerene and to the second reduction of NBP, respectively (Figure 2 and Table 1). Compounds **1a**–**f** display reduction waves that are shifted to more negative potentials relative to those of parent C_{60}.[28–30] This is in line with other CV studies performed on fulleropyrrolidines and is a consequence of the saturation of the double bond.[10,17,28,30–32]

The linear relationship existing between peak current and the square root of the scan rate between 0.01–1 V s^{-1} (correlation coefficient about 0.99) shows that the electrochemical processes are predominantly diffusion controlled in the entire scan rate range studied. Also, the value of ΔE between the oxidation and reduction peaks remains constant as the scan rate is increased, so the electrochemical processes are reversible.[33]

Supramolecular Assemblies of Fulleropyrrolidine-Based Dyads

Fulleropyrrolidine–phthalimide dyads **1a**–**f** were found to be stable under normal ambient conditions for prolonged periods of time. These compounds are readily soluble in chloroform, dichloromethane, tetrahydrofuran, DMF, dioxane, and toluene (20 mg mL^{-1}) and sparingly soluble in methanol and isopropanol (5 mg mL^{-1}). To assess the aggregation capabilities of **1a**–**f**, we performed DOSY NMR analyses[34,35] in $CDCl_3$, and on the basis of the obtained diffusion coefficients, we calculated their hydrodynamic radii by using the Stokes–Einstein equation.[36] At a concentration of 2 mM, the hydrodynamic radii of all derivatives were between 5.1–6.2 Å, which indicates that there was no aggregation under the conditions tested. In comparison, the radius for parent C_{60} is 5.003 Å.[36]

Supramolecular assemblies of **1a**–**f** were obtained by employing the drop-drying or facile solvent evaporation method[22,23] by using various sample preparation conditions. All compounds showed solvent- and temperature-induced polymorphism. Solvents and solvent systems with variable polarities used in these experiments were toluene, dioxane, methanol, toluene/dioxane (2:1), toluene/isopropanol (1:1 and 2:1), and chloroform/methanol (2:1). Additionally, the structures of the dyads themselves influenced their supramolecular arrangements. In this way, varying the length of the spacer in **1a**–**f** yielded various morphologies, exhibiting so-called supramolecular shape-shifting. This phenomenon was also observed by Nakanishi and coworkers.[37–39]

As depicted in the SEM images, well-defined architectures were observed for **1a** (Figure 3) and **1b**, whereas less-ordered self-assembly was observed for **1c**–**f** (for additional images see the Supporting Information).

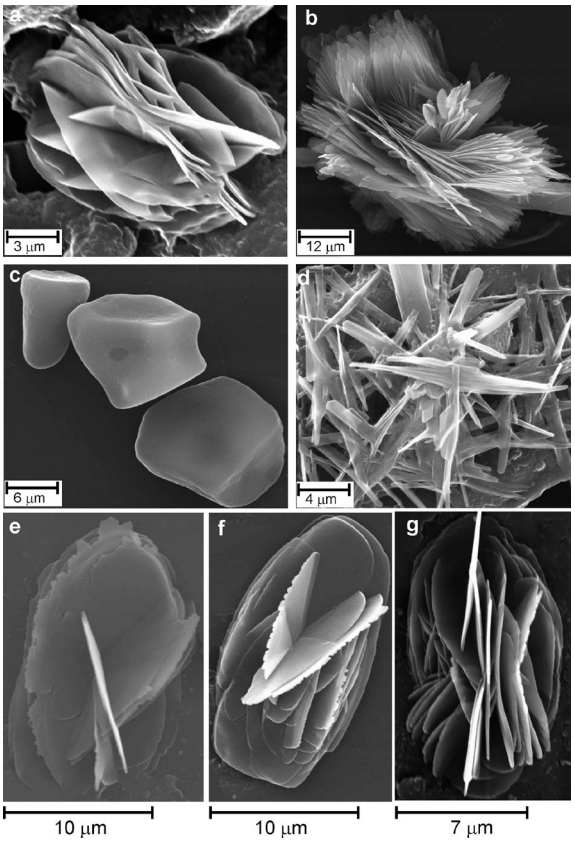

Figure 3. SEM images of **1a** prepared from (a) dioxane, (b) toluene/isopropanol mixture (1:1), (c) toluene (rapid cooling), (d) toluene (incubation at –20 °C), and (e–g) toluene/isopropanol mixture (2:1).

Fulleropyrrolidine **1a** exhibited exceptionally good self-assembly properties in all solvent systems and for all sample preparation methods used (Figure 3). In all cases, fulleropyrrolidine **1a** (1 mg) was dissolved in the solvent (1 mL) and heated at 60 °C for 2 h. When dioxane and toluene/isopropanol (1:1) were used, the sample was gradually cooled to room temperature over 24 h. A drop of the solution was then applied onto a Si wafer by using a capillary, and the solvent was slowly evaporated at room temperature prior to SEM analysis. Under these conditions, flower-shaped assemblies were observed (Figure 3, a,b). When toluene was used as the solvent under different cooling conditions, **1a** arranged into different supramolecular assemblies. Thus, rapid cooling resulted in objects with a less-ordered architecture (Figure 3, c), whereas aging at room temperature for 24 h followed by incubation at –20 °C for 12 h resulted in rod-shaped structures (Figure 3, d). When toluene/isopropanol (2:1) was used, flower-like architectures of **1a** were obtained. Images of semiformed superstructures provided insight to its mechanism of formation (Figure 3, e–g). The first step was the formation of microplates (Figure 3, e), which under slow evaporation had the tendency to coalesce together (Figure 3, e,f). Finally, these micrometer-sized petal-like objects formed flower-shaped morphologies with a final size of 10–17 μm (Figure 3, g).

It could be assumed that the observed self-assembly process was possibly driven by π–π interactions of the C_{60} and phthalimide moieties, as well as by van der Waals interactions of the aliphatic chain spacer, which would enable the oriented attachment and growth of the microplates. Flower-shaped assemblies are often observed in hierarchical organization of fullerene derivatives.[37,40]

Derivative **1b** assembled in globular structures of dense microflakes when the toluene solution was kept at –20 °C for 12 h prior to SEM examination (see the Supporting Information). However, without freezing, **1b** exhibited less-ordered self-assembly of the microflakes. The beginnings of a supramolecular architecture were detected when toluene/isopropanol (2:1) was used. As already mentioned, compounds **1c**–**f** having increased lengths of the alkyl spacers showed less-ordered architectures under the examined experimental conditions and formed nanospherical self-assembled structures. The observed trend could be the result of an increased relative influence of the van der Waals interactions associated with alkyl chains.

Conclusions

Herein we described the synthesis and properties of newly designed fulleropyrrolidine derivatives **1a**–**f** consisting of two electron-acceptor moieties (fullerene and phthalimide) joined by a nonpolar alkyl linker (C_2–C_{12}). Their synthesis was significantly improved by microwave-assisted coupling of phthalimide and the corresponding fulleroamines. The electrochemical properties of the fullerene–phthalimide dyads were notably influenced by the distance of the acceptor moieties. Micrometer-sized self-arranged supramolecular objects were obtained by drop-drying methods, and supramolecular shape-shifting occurred with increasing length of the hydrophobic spacer, which was probably controlled by a fine balance between π–π and van der Waals interactions.

Experimental Section

General Methods: FTIR spectra were recorded with a Perkin–Elmer FTIR 1725X spectrophotometer. ^{1}H NMR and ^{13}C NMR spectra were recorded with Varian Gemini 200 and Bruker Avance III 500 spectrometers at 200/50 and 500/125 MHz, respectively. The chemical shifts were measured to residual non-deuterated solvent resonances or tetramethylsilane. Fullerenic carbon atoms, presented as C_f, were numbered in a simplified way, according to the literature.[41] Mass spectra were obtained with an Agilent Technologies 6210 TOF LC–MS instrument. UV spectra were recorded with a GBC-Cintra 40 spectrophotometer. Reactions were monitored by TLC by using plates precoated with silica gel 60 F254. Column chromatography was performed on silica gel, 10–18, 60A, ICN Biomedicals. Standard techniques were used for the purification of the reagent and solvents.[42] Reactions induced by microwave irradiation were performed in a Milestone MultiSynth microwave multimode oven by using a MedCHEM kit and MonoPREP kit.

Electrochemical Measurements: The electrochemical behaviors of the fullerophthalimide dyads were investigated by using 1 mM solutions of compounds **1a–f** in dry DMF containing 0.1 M nBu_4NPF_6 as the supporting electrolyte. To remove oxygen from the electrolyte, the system was bubbled with nitrogen prior to each experiment. The nitrogen inlet was then moved above the liquid surface and left there during the scans. The electrochemical measurements were carried out with a CHI760b Electrochemical Workstation potentiostat (CH Instruments, Austin, TX) by using a conventional three-electrode cell (1 mL) equipped with a glassy carbon electrode as the working electrode, a Ag/Ag^+ electrode (a silver wire in contact with 0.01 M $AgNO_3$ and 0.10 M nBu_4NPF_6 in DMF) as the reference electrode, and a platinum wire as the auxiliary electrode, calibrated with the ferrocene/ferrocenyl couple (Fc/Fc^+) as an internal standard. All experiments were performed at room temperature in the potential range of –3.3 to 0.0 V vs. Fc/Fc^+ at sweep rates between 0.01 and 1 V cm^{-1}.

Morphology Measurements: Investigation of the morphologies of the samples were carried out by scanning electron microscopy with a JEOL JSM-840A instrument at an acceleration voltage of 30 kV. Several drops of a dilute solution [ca. 1 mM in toluene, dioxane, methanol, toluene/dioxane (2:1), toluene/isopropanol (1:1 and 2:1), and chloroform/methanol (2:1)] of the fullerophthalimide dyads were deposited on the surface of a Si wafer and then slowly evaporated in a glass petri dish (diameter 10 cm) under a toluene atmosphere at room temperature. The investigated samples were gold sputtered in a JFC 1100 ion sputterer and then subjected to SEM observations.

General Procedure for the Preparation of Fulleropyrrolidine–Phthalimide Dyads 1a–f: A suspension of **6a–f** (0.015 mmol) and phthalic anhydride (0.015 mmol equiv.) in AcOH/pyridine (3:2, 1 mL) was irradiated in a microwave reactor for 30 min with an inner temperature of 130 °C and an applied pulse of 300 W. The obtained reaction mixture was evaporated to dryness, and the excess amount of acetic acid was removed by coevaporation with toluene. The crude product was purified by column chromatography on SiO_2 (EtOAc/toluene, 9:1). Subsequent precipitation by adding MeOH to a highly concentrated solution of the product in CH_2Cl_2/CS_2 gave pure products **1a–f** as brown powders in 40–59% yield.

1a: Yield 8.3 mg (59%). UV/Vis (CH_2Cl_2): λ_{max} (ε, $M^{-1}cm^{-1}$) = 254 (120000), 308 (48000), 320 (55000), 431 (4600), 704 nm (650). IR (ATR): $\tilde{\nu}$ = 3464, 2926, 1711, 1391, 717 cm^{-1}. ^1H NMR (500 MHz, $CDCl_3$): δ = 7.89–7.87 (m, 2 H), 7.73–7.71 (m, 2 H), 4.48 (s, 4 H), 4.27 (t, J = 6 Hz, 2 H), 3.47 ppm (t, J = 6 Hz, 2 H). ^{13}C NMR (120 MHz, $CDCl_3$): δ = 168.5 (2 C), 154.7 (C_f-12), 147.2 (C_f-17), 146.2 (C_f-7), 146.1 (C_f-11), 146.0 (C_f-16), 145.3 (C_f-5), 145.2 (C_f-9), 144.5 (C_f-15), 143.0 (C_f-8), 142.5 (C_f-6), 142.1 (C_f-14), 142.0 (C_f-4), 141.8 (C_f-12, C_f-13), 140.0 (C_f-10), 136.1 (C_f-3), 133.9 (2 C), 132.3 (2 CH), 123.4 (2 CH), 70.6 (2 C), 67.8 (2 CH_2), 50.9 (CH_2), 36.6 ppm (CH_2). HRMS: calcd. for $[C_{72}H_{12}N_2O_2 + H]^+$ 937.0971; found 937.0993.

1b: Yield 5.8 mg (40%). UV/Vis (CH_2Cl_2): λ_{max} (ε, $M^{-1}cm^{-1}$) = 253 (130000), 309 (49000), 321 (56000), 430 (4800), 703 nm (700). IR (ATR): $\tilde{\nu}$ = 3453, 2927, 2854, 1710, 1395, 710 cm^{-1}. ^1H NMR (200 MHz, $CDCl_3$): δ = 7.88–7.82 (m, 2 H), 7.75–7.69 (m, 2 H), 4.38 (s, 4 H), 3.88 (t, J = 6 Hz, 2 H), 3.13 (t, J = 6 Hz, 2 H), 2.08–1.94 ppm (m, 4 H). ^{13}C NMR (50 MHz, $CDCl_3$): δ = 163.5 (2 C), 154.8 (C_f-12), 146.1 (C_f-11), 145.9 (C_f-16), 145.3 (C_f-5), 145.1 (C_f-9), 144.4 (C_f-15), 143.0 (C_f-8), 142.5 (C_f-6), 142.1 (C_f-14), 141.9 (C_f-4), 141.7 (C_f-12,13), 140.0 (C_f-10), 136.1 (C_f-3), 133.7 (2 C), 132.1 (2 CH), 123.0 (2 CH), 70.4 (2 C), 67.7 (2 CH_2), 54.1 (CH_2), 37.6 (CH_2), 26.6 (CH_2), 26.0 ppm (CH_2). HRMS: calcd. for $[C_{74}H_{16}N_2O_2 + H]^+$ 965.1284; found 965.1285. HRMS: calcd. for $[M + H]^+$ 965.1284; found 965.1285.

1c: Yield 7.5 mg (51%). UV/Vis (CH_2Cl_2): λ_{max} (ε, $M^{-1}cm^{-1}$) = 253 (118000), 308 (47000), 320 (56000), 430 (4900), 703 nm (500). IR (ATR): $\tilde{\nu}$ = 3442, 2928, 2852, 1688, 1521, 718 cm^{-1}. ^1H NMR (200 MHz, $CDCl_3$): δ = 7.87–7.81 (m, 2 H); 7.76–7.69 (m, 2 H), 4.39 (s, 2 H), 3.77 (t, J = 7.2 Hz, 2 H), 3.08 (t, J = 7.2 Hz, 2 H), 1.95–1.46 ppm (m, 12 H). ^{13}C NMR (50 MHz, $CDCl_3$): δ = 167.8 (2 C), 155.1 (C_f-12), 147.3 (C_f-17), 146.2 (C_f-7), 146.0 (C_f-11), 145.4 (C_f-16), 145.2 (C_f-5), 145.1 (C_f-9), 144.5 (C_f-15), 143.0 (C_f-8), 142.5 (C_f-6), 142.2 (C_f-14), 142.0 (C_f-4), 141.8 (C_f-12,13), 140.1 (C_f-10), 136.2 (C_f-3), 133.8 (2 C), 132.1 (2 CH), 123.2 (2 CH), 70.6 (2 C), 67.9 (2 CH_2), 54.9 (CH_2), 37.9 (CH_2), 28.6 (2 CH_2), 27.2 (CH_2), 26.8 ppm (CH_2). HRMS: calcd. for $[C_{76}H_{20}N_2O_2 + H]^+$ 993.1597; found 993.1593.

1d: Yield 6.9 mg (45%). UV/Vis (CH_2Cl_2): λ_{max} (ε, $M^{-1}cm^{-1}$) = 254 (130000), 310 (50000), 322 (56000), 432 (5100), 704 nm (700). IR (ATR): $\tilde{\nu}$ = 3457, 2925, 2851, 1711, 1393, 717 cm^{-1}. ^1H NMR (200 MHz, $CDCl_3$): δ = 7.86–7.79 (m, 2 H), 7.74–7.66 (m, 2 H), 4.39 (s, 4 H), 3.71 (t, J = 7.6 Hz, 2 H), 3.06 (t, J = 7.6 Hz, 2 H), 2.03–1.86 (2 H), 1.80–1.39 ppm (m, 4 H). ^{13}C NMR (50 MHz, $CDCl_3$): δ = 168.3 (2 C), 155.1 (C_f-12), 147.2 (C_f-17), 146.2 (C_f-7), 146.1 (C_f-11), 145.9 (C_f-16), 145.6 (C_f-5), 145.3 (C_f-9), 145.2 (C_f-15), 144.5 (C_f-8), 142.5 (C_f-6), 142.2 (C_f-14), 142.0 (C_f-4), 141.8 (C_f-12,13), 140.1 (C_f-10), 136.2 (C_f-3), 133.8 (2 C), 132.2 (2 CH), 123.1 (2 CH), 70.6 (2 C), 67.9 (2 CH_2), 55.1 (CH_2), 37.9 (CH_2), 29.5 (2 CH_2), 29.2 (2 CH_2), 28.8 (CH_2), 28.6 (CH_2), 27.6 (CH_2), 26.8 ppm (CH_2). HRMS: calcd. for $[C_{78}H_{24}N_2O_2 + H]^+$ 1021.1910; found 1021.1912.

1e: Yield 9.1 mg (58%). UV/Vis (CH_2Cl_2): λ_{max} (ε, $M^{-1}cm^{-1}$) = 252 (125000), 308 (47000), 322 (54000), 432 (4800), 704 nm (600). IR (ATR): $\tilde{\nu}$ = 3464, 2926, 2851, 1711, 1394, 718 cm^{-1}. ^1H NMR (200 MHz, $CDCl_3$): δ = 7.86–7.75 (m, 2 H), 7.72–7.68 (m, 2 H), 4.40 (s, 4 H), 3.69 (t, J = 7.5 Hz, 2 H), 3.07 (t, J = 7.5 Hz, 2 H), 2.01–1.86 (m, 2 H), 1.72–1.24 ppm (m, 14 H). ^{13}C NMR (50 MHz, $CDCl_3$): δ = 168.3 (2 C), 155.1 (C_f-12), 147.2 (C_f-17), 146.2 (C_f-7), 146.1 (C_f-11), 146.0 (C_f-16), 145.4 (C_f-5), 145.3 (C_f-9), 145.2 (C_f-15), 144.5 (C_f-8), 142.5 (C_f-6), 142.2 (C_f-14), 142.0 (C_f-4), 141.8 (C_f-12,13), 140.1 (C_f-10), 136.2 (C_f-3), 133.8 (2 C), 132.2 (2 CH), 123.1 (2 CH), 70.6 (2 C), 67.9 (2 CH_2), 55.1 (CH_2), 38.0 (CH_2), 29.6 (CH_2), 29.5 (CH_2) 29.2 (2 CH_2), 28.9 (CH_2), 28.6 (CH_2), 27.0 (CH_2), 26.9 ppm (CH_2). HRMS: calcd. for $[C_{80}H_{28}N_2O_2 + H]^+$ 1049.2223; found 1049.2234.

1f: Yield 9.2 mg (57%). UV/Vis (CH_2Cl_2): λ_{max} (ε, $M^{-1}cm^{-1}$) = 253 (118000), 309 (49000), 320 (54000), 431 (4800), 703 nm (540). IR (ATR): $\tilde{\nu}$ = 3662, 2926, 2855, 1688, 1386, 720 cm^{-1}. ^1H NMR (200 MHz, $CDCl_3$): δ = 7.85–7.83 (m, 2 H), 7.71–7.69 (m, 2 H), 4.41 (s, 4 H), 3.68 (t, J = 7.4 Hz, 2 H), 3.08 (t, J = 7.4 Hz, 2 H), 1.98–1.92 (2 H), 1.69–1.59 (m, 4 H), 1.51–1.45 (2 H), 1.45–1.32 ppm (12 H). ^{13}C NMR (50 MHz, $CDCl_3$): δ = 168.5 (2 C), 155.2 (C_f-12), 147.3 (C_f-17), 146.2 (C_f-7), 146.1 (C_f-11), 146.0 (C_f-16), 145.7 (C_f-5), 145.4 (C_f-9), 145.3 (C_f-15), 144.6 (C_f-8), 142.6 (C_f-6), 142.3 (C_f-14), 142.1 (C_f-4), 141.9 (C_f-12,13), 140.1 (C_f-10), 136.2 (C_f-3), 133.8 (2 C), 132.2 (2 CH), 123.1 (2 CH), 70.7 (2 C), 68.0 (2 CH_2), 55.2 (CH_2), 38.1 (CH_2), 29.6 (3 CH_2), 29.5 (CH_2), 29.2 (2 CH_2), 28.8 (CH_2), 28.6 (CH_2), 27.7 (CH_2), 26.9 ppm (CH_2). HRMS: calcd. for $[C_{82}H_{32}N_2O_2 + H]^+$ 1077.2536; found 1077.2550.

Supporting Information (see footnote on the first page of this article): Experimental details and spectroscopic data for **1–5**; additional SEM images of **1b–f**; ^1H NMR and ^{13}C NMR spectra of **1a–f**, **2b–f**, **3b–f**, **4b–f**, and **5b–f**.

Acknowledgments

Financial support of the Ministry of Education, Science and Technological Development of the Republic of Serbia is acknowledged (project number 172002).

[1] H. W. Kroto, J. R. Heath, S. C. O'Brien, R. F. Curl, R. E. Smalley, *Nature* **1985**, *318*, 162–163.
[2] W. Kratschmer, L. D. Lamb, K. Fostriropoulos, D. R. Huffman, *Nature* **1990**, *347*, 354–358.
[3] K. Kordatos, T. Da Ros, S. Bosi, E. Vasquez, M. Bergamin, C. Cusan, F. Pellarini, V. Tomberli, B. Baiti, D. Pantarotto, V. Georgakilas, G. Spalluto, M. Prato, *J. Org. Chem.* **2001**, *66*, 4915–4920.
[4] M. Maggini, G. Scorrano, M. Prato, *J. Am. Chem. Soc.* **1993**, *115*, 9798–9799.
[5] M. Prato, M. Maggini, *Acc. Chem. Res.* **1998**, *31*, 519–526.
[6] T. Da Ros, M. Bergamin, E. Vasquez, G. Spalluto, B. Baiti, S. Moro, A. Boutorine, M. Prato, *Eur. J. Org. Chem.* **2002**, 405–413.
[7] M. Bjelaković, N. Todorović, D. Milić, *Eur. J. Org. Chem.* **2012**, 5291–5300.
[8] L. Echegoyen, L. E. Echegoyen, *Acc. Chem. Res.* **1998**, *31*, 593–601.
[9] B. M. Illescas, N. Martin, in: *Handbook of Nanophysics: Clusters and Fullerenes* (Ed.: K. D. Sattler), CRC Press, Boca Raton, **2011**, vol. 36, pp. 36.1–36.16.
[10] B. M. Illescas, N. Martin, *C. R. Chim.* **2006**, *9*, 1038–1050.
[11] N. Martin, L. Sanchez, B. Illescas, I. Peres, *Chem. Rev.* **1998**, *98*, 2527–2547.
[12] B. M. Illescas, N. Martin, *J. Org. Chem.* **2000**, *65*, 5986–5995.
[13] J. Ortiz, F. Fernandez-Lazaro, A. Sastre-Santos, J. A. Quintana, J. M. Villalvilla, M. A. Diaz-Garcia, J. A. Rivera, S. E. Stepleton, C. T. Cox Jr., L. Echegoyen, *Chem. Mater.* **2004**, *16*, 5021–5026.
[14] M. K. Kashavarz, B. Knight, R. C. Haddon, F. Wudl, *Tetrahedron* **1996**, *52*, 5149–5159.
[15] T. Nakanishi, *Chem. Commun.* **2010**, *46*, 3425–3436.
[16] S. S. Babu, H. Mohwald, T. Nakanishi, *Chem. Soc. Rev.* **2010**, *39*, 4021–4035.
[17] M. Prato, *J. Mater. Chem.* **1997**, *7*, 1097–1109.
[18] A. M. Lopez, A. Mateo-Alonso, M. Prato, *J. Mater. Chem.* **2011**, *21*, 1305–1318.
[19] S. S. Gayathri, A. K. Agarwal, K. A. Suresh, A. Patnaik, *Langmuir* **2005**, *21*, 12139–12145.
[20] S. S. Gayathri, A. Patnaik, *Langmuir* **2007**, *23*, 4800–4808.
[21] H. Asanuma, H. Li, T. Nakanishi, H. Mohwald, *Chem. Eur. J.* **2010**, *16*, 9330–9338.
[22] L. Wang, B. Liu, S. Yu, M. Yao, D. Liu, Y. Hou, T. Cui, G. Zou, *Chem. Mater.* **2006**, *18*, 4190–4194.
[23] C. Park, H. J. Song, H. C. Choi, *Chem. Commun.* **2009**, 4803–4805.
[24] P. de la Cruz, A. de la Hoz, F. Langa, *Tetrahedron* **1997**, *53*, 2599–2608.
[25] F. Langa, P. de la Cruz, *Comb. Chem. High Throughput Screening* **2007**, *10*, 766–782.
[26] I. Guryanov, A. M. Lopez, M. Carraro, T. Da Ros, G. Scorrano, M. Maggani, M. Prato, M. Bonchio, *Chem. Commun.* **2009**, 3940–3942.
[27] S. Filippone, M. I. Barros, A. Martin-Domenech, S. Osuna, S. Miquel, N. Martin, *Chem. Eur. J.* **2008**, *14*, 5198–5206.
[28] T. Suzuki, Y. Maruyama, T. Akasaka, W. Ando, K. Kobayashi, S. Nagase, *J. Am. Chem. Soc.* **1994**, *116*, 1359–1363.
[29] T. Da Ros, M. Prato, M. Carraro, P. Ceroni, F. Paolucci, S. Roffia, *J. Am. Chem. Soc.* **1998**, *120*, 11645–11648.
[30] M. Wielopolski, G. de Miguel Rojas, C. Van der Pol, L. Brinkhaus, G. Katsukis, M. R. Bryce, T. Clark, D. M. Guldi, *ACS Nano* **2010**, *4*, 6449–6462.
[31] G. de Miguel, M. Wielopolski, D. I. Schuster, M. A. Fazio, O. P. Lee, C. K. Haley, A. L. Ortiz, L. Echegoyen, T. Clark, D. M. Guldi, *J. Am. Chem. Soc.* **2011**, *133*, 13036–13054.
[32] F. Scarel, G. Valenti, S. Gaikwad, M. Marcaccio, F. Paolucci, A. Mateo-Alonso, *Chem. Eur. J.* **2012**, *18*, 14063–14068.
[33] A. J. Bard, L. R. Faulkner, *Electrochemical Methods: Fundamentals and Applications*, 2nd ed., John Wiley & Sons, Inc., New York, **2001**.
[34] Y. Cohen, L. Avram, L. Frish, *Angew. Chem.* **2005**, *117*, 524; *Angew. Chem. Int. Ed.* **2005**, *44*, 520–554.
[35] Y. Y. Zhu, C. Li, G. Y. Li, X. K. Jiang, Z. T. Li, *J. Org. Chem.* **2008**, *73*, 1745–1751.
[36] R. Haselmeier, M. Holz, M. M. Kappes, R. H. Michel, D. Fuchs, *Ber. Bunsen-Ges.* **1994**, *98*, 878–881.
[37] T. Nakanishi, K. Ariga, T. Michinobu, K. Yoshida, H. Takahashi, T. Teranishi, H. Mohwald, D. G. Kurth, *Small* **2007**, *3*, 2019–2023.
[38] T. Nakanishi, W. Schmittt, T. Michinobu, D. G. Kurth, K. Ariga, *Chem. Commun.* **2005**, 5982–5984.
[39] T. Nakanishi, J. Wang, H. Mohwald, D. G. Kurt, T. Michinobu, M. Takeuchi, K. Ariga, *J. Nanosci. Nanotechnol.* **2009**, *9*, 550–556.
[40] Y. Xiao, M. Zhang, F.-X. Wang, G.-B. Pan, *CrystEngComm* **2012**, *14*, 1933–1935.
[41] M. S. Meier, H. P. Spielmann, R. G. Bergosh, M. C. Tetreau, *J. Org. Chem.* **2003**, *68*, 7867–7870.
[42] D. D. Perrin, W. L. Armarego, *Purification of Laboratory Chemicals*, 3rd ed., Pergamon Press, Oxford, New York, **1988**.

Received: December 4, 2012
Published Online: February 20, 2013

